UHV Study of Hydrogen Atom Induced Etching of Amorphous Hydrogenated Silicon Thin Films

Thomas Zecho[†], Birgit D. Brandner[†], Jürgen Biener,*[,‡] and Jürgen Küppers[†,‡]

Experimentalphysik III, Universität Bayreuth, 95440 Bayreuth, Germany, and Max-Planck-Institut für Plasmaphysik (EURATOM Association), 85748 Garching, Germany

Received: June 22, 2000; In Final Form: November 9, 2000

Amorphous hydrogenated silicon (a-Si:H) films were deposited at 300 K by the ion-beam-deposition (IBD) method on a Pt(111) single crystal and characterized by means of Auger electron spectroscopy (AES), electronic and vibrational electron energy loss spectroscopy (EELS, HREELS), and thermal desorption spectroscopy (TDS). The a-Si:H films appear to grow in a two-dimensional mode, and exhibit a polymer-like structure with a hydrogen content of approximately 45 at. %, bonded in monohydride (SiH) and dihydride (SiH_2) groups. The films are stable up to 500 K; above this temperature the evolution of hydrogen and the formation of platinum silicides were observed. Exposure to atomic hydrogen leads to the formation of silane, disilane, and higher silicon hydrides. Between 100 and 300 K a constant etching rate of Si/H = ∼0.01 was observed. At higher temperatures the etching rate decreased due to the beginning instability of higher hydrides and the competing process of silicide formation.

1. Introduction

Amorphous hydrogenated silicon (a-Si:H) is used for the fabrication of flat-panel displays[1] and solar cells[2] due to the possibility of producing large-area, low-cost semiconducting films. Device-quality a-Si:H films are usually deposited by plasma-enhanced chemical vapor deposition (PECVD) from a silane plasma on a substrate held at 250−400 °C.[3] Besides the substrate temperature, the interaction of hydrogen atoms with a-Si:H plays an important role during deposition which allows adjustment of the desired properties of the material, such as high photoconductivity-to-dark conductivity ratio, low dangling bond density, and improved stability under light irradiation. The impact of hydrogen on the properties of a-Si:H can be influenced by hydrogen dilution of the SiH_4 plasma,[4] thereby modifying both plasma chemistry and surface reactions. An alternative approach is the postdeposition treatment of a-Si:H films with atomic hydrogen,[5] which is called "chemical annealing".[6−8] Both techniques allow growth of microcrystalline silicon (μc-Si:H) films at low substrate temperatures.[4,9,10]

Possible interactions of hydrogen atoms with silicon-based materials include hydrogen abstraction, hydrogenation of dangling bonds, insertion of hydrogen into the Si−Si bonds, and chemical etching. The etching reaction is generally explained in terms of a sequence of insertion and hydrogenation reactions, finally leading to the formation of volatile products. The formation of silane has been observed in the interaction of hydrogen atoms with both amorphous[11,12] and crystalline[13−18] silicon. The formation of silane was proposed to proceed via hot atom or Eley−Rideal type reactions between silyl ($-SiH_3$) surface groups and impinging hydrogen atoms.[12,17,18] However, contradictory results regarding the temperature dependence of the etching reaction have been reported: Chiang et al.[19] observed a fast etching reaction at 473 K, but very slow etching at 163 K, whereas Olander et al.[13] reported a decrease of the etching rate with increasing temperature. In another study, Jo et al.[17] pointed out that the rate of the hydrogen induced etching of silicon is controlled by both the formation and the abstraction of silyl; while the formation of silane via the hydrogen induced abstraction of silyl increased with increasing temperature, just the opposite has been observed for the formation of silyl groups via insertion and hydrogenation reactions due to the low thermal stability of silyl.

In the present work, we investigated both the deposition and the hydrogen induced etching of a-Si:H films. The films were deposited on a Pt(111) substrate using the ion-beam-deposition (IBD) method. A metallic substrate was selected, because it makes easier the temperature control during deposition and erosion as well as the use of electron spectroscopies. All films were deposited at 300 K to exclude the formation of platinum silicides. Due to the low deposition temperature, the a-Si:H films were hydrogen-rich and exhibit a polymer-like structure. In this study we were specifically interested in the temperature dependence and the product distribution of the etching reaction.

2. Experimental Section

The present study was performed in an ultrahigh vacuum (UHV) system with a base pressure of 5×10^{-11} Torr. The instrumentation for HREELS and AES is located in separate, individually pumped compartments, which are connected via gate valves to the preparation chamber. The hydrogen atom source is installed into a small, differentially pumped vacuum system (source chamber), which also houses the quadrupole mass spectrometer (QMS). The source chamber is connected through a small aperture of 8 mm diameter to the preparation chamber. The aperture can be closed with a mechanical shutter, which allows to maintain a pressure gradient of 3 orders between the source chamber and the preparation chamber. The QMS and the surface surrounding the atom source were thus protected from disilane exposure during the film deposition.

* Corresponding author. E-mail: juergen.biener@uni-bayreuth.de. Telephone: +49 921-553809. FAX: +49 921-553802.

† Experimentalphysik III, Universität Bayreuth, 95440 Bayreuth, Germany.

‡ Max-Planck-Institut für Plasmaphysik (EURATOM Association), 85748 Garching, Germany.

10.1021/jp0022611 CCC: $20.00
Published on Web 04/04/2001

During the reaction measurements the sample was placed just in front of the aperture and the exposure to hydrogen atoms was controlled by means of the mechanical shutter.

The hydrogen atoms are generated in a resistively heated tungsten tube. To determine the flux of hydrogen atoms at the sample, both the total flux and the angular distribution of the hydrogen atoms have to be known. The total flux of atoms was determined from the hydrogen gas throughput and the temperature of the tungsten tube at the front end, and the angular distribution of the atoms was measured following the approach of Schwarz-Selinger et al.[20] In short, the hydrogen atom induced chemical erosion of an amorphous hydrogenated carbon film is used to determine the angular distribution of the hydrogen atoms from the measured spatial variation of the erosion rate. In the present study a hydrogen flow of 0.45 sccm and a tungsten tube temperature of 2200 K were used, resulting in an atom flux of $\sim 10^{16}$ H cm^{-2} s^{-1}.

The a-Si:H films investigated in the present study were deposited by the ion-beam-deposition (IBD) method. The ion gun operated at an ion energy of 180 eV in a disilane (Si_2H_6) ambient of 5×10^{-5} Torr. During the deposition an ion current of approximately 1 μA was measured, and used to monitor the film growth. The films were deposited on a Pt(111) single crystal, which was mounted via two tungsten wires to a precision manipulator. The substrate temperature was measured by means of a chromel/alumel thermocouple attached to the Pt crystal. Resistive heating and cryocooling allows adjustment of sample temperatures between 80 and 1400 K. Prior to each deposition of a-Si:H, the Pt surface was cleaned by standard procedures.[21] All a-Si:H films investigated in the present work were deposited at 300 K.

To investigate the rate of the etching reaction, the partial pressures of silane, disilane, and higher silane species were continuously monitored while exposing the a-Si:H films to hydrogen atoms. The samples were first positioned in front of the aperture of the source chamber with the atom source working and the shutter closed, and then the hydrogen exposure was started by opening of the shutter at $t = 0$ s. The measurements were continued until the a-Si:H films were completely etched away as indicated by the vanishing product signal. Both the sensitivity of the QMS and the pumping speed of the products in the source chamber were determined, thus allowing conversion of the measured signals into rates of formation. The fragmentation patterns of silane and disilane were measured, and were shown to be in good agreement with the literature[22,23] (with the exception of disilane in the presence of hydrogen atoms, see discussion below).

3. Results and Discussion

3.1. Characterization of the a-Si:H Films.

The growth of a-Si:H films was monitored by means of AES (Figure 1). To assess the deposition rate, the AES peak ratio Si_{92}/Pt_{64} was measured as a function of the deposition time (Figure 1, insert). The thickness of the a-Si:H films was estimated using the attenuation lengths from the universal mean free path curve,[24] revealing a deposition rate of approximately 10 nm/h. This simple analysis may lead to significant errors in determining the growth rate due to the possible formation of silicides at the Pt/a-Si:H interface.[25,26] However, the growth rate was confirmed by a calculation using the integrated ion current monitored during deposition, and assuming that $Si_2H_y^+$ ions with a sticking coefficient of unity are responsible for the film growth. The integrated QMS signals of silane species, measured during the complete erosion of the a-Si:H films, are consistent with

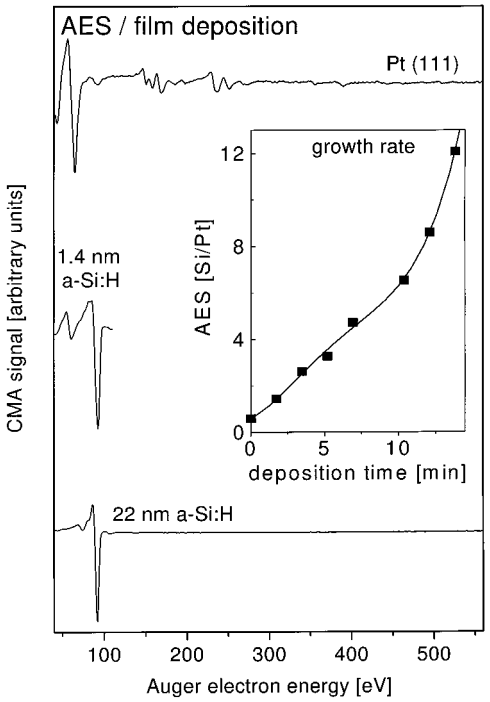

Figure 1. AES spectra of the clean Pt(111) surface, and after deposition of 1.4 and 22 nm thick a-Si:H films, respectively. The inset shows the AES peak ratio Si_{92}/Pt_{64} as a function of the deposition time.

the film thickness calculated from the growth rate and the deposition time. The Pt_{64} AES signal decreases with increasing deposition time, until the detection limit is reached after approximately 25 min. A comparison with the integrated ion current used as a monitor of the deposited amount of Si atoms suggests the growth of a continuous a-Si:H film. The rapid attenuation of the Pt_{64} signal in the initial growth regime further indicates that the deposited a-Si:H films are stable at 300 K, and do not react with the Pt substrate toward a silicide phase. However, the formation of a thin silicide interface layer cannot be excluded. The formation of such a silicide interface structure with a thickness of 2 nm was reported for the deposition of Pd on a-Si:H at 300 K.[27] Oxygen and carbon contaminations were always below the AES detection limit.

To assess the density of the deposited a-Si:H, EELS spectra were collected from a 24 nm thick a-Si:H film as a function of the primary electron energy (Figure 2). The loss peaks at 16.7 and 9.5 eV can be assigned to volume and surface plasmons of a-Si:H, respectively.[28,29] Consistent with this assignment, the ratio of the intensities $I_{surface}/I_{bulk}$ increases with decreasing energy of the incident electrons. The broad feature observed at higher energies can be assigned to multiple excitations. The correlation between plasmon energy and electron density[24] allows estimation of the specific gravity of the deposited a-Si:H films. On clean Si(111) 7×7 the bulk plasmon has been observed at 17.5 eV.[29] The density of the investigated a-Si:H films thus seems to be only 10% lower than that of crystalline silicon, neglecting the hydrogen contribution to the electron density in a first approximation. However, the density of hydrogen-rich a-Si:H films deposited at room temperature has been reported to be up to 30% lower than that of crystalline silicon.[30] The relatively high value of the EELS-derived density of a-Si:H in the present work thus seems to reflect the inaccuracy of the method.

To investigate the thermal stability of the a-Si:H films deposited on a Pt(111) surface, an annealing experiment was performed with a 3 nm thick a-Si:H film (Figure 3). The

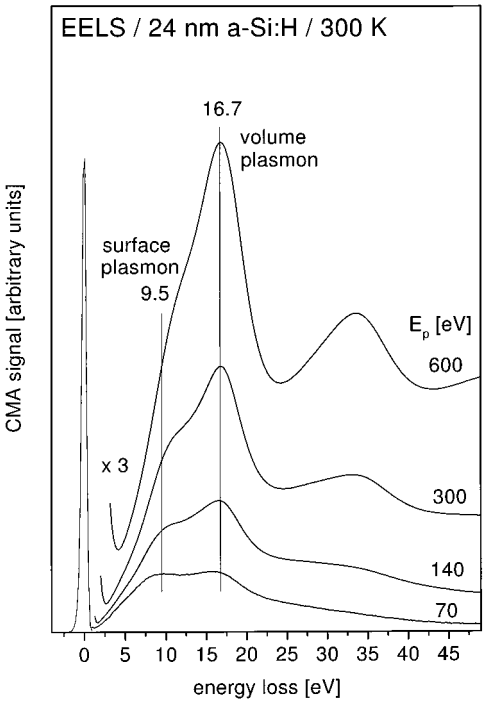

Figure 2. EELS spectra of a 24 nm thick a-Si:H film as a function of primary electron energy.

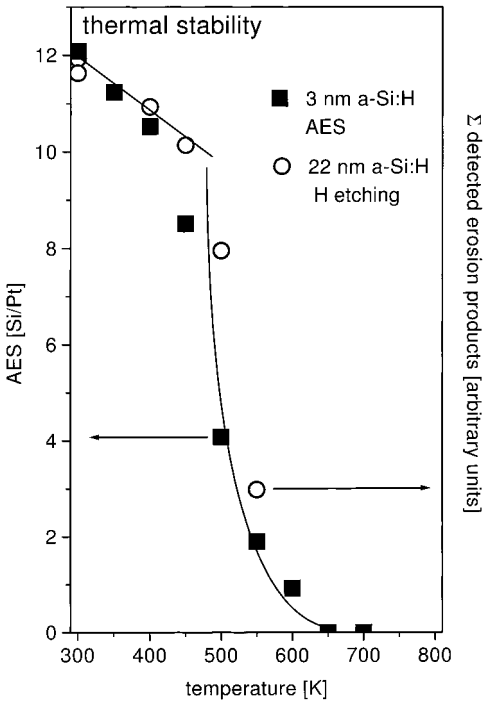

Figure 3. Variation of the AES peak ratio Si_{92}/Pt_{64} of an initially 3 nm thick a-Si:H film as a function of annealing temperature (solid squares). Also shown is total yield of silicon atoms detected in the etch product channels during the complete erosion of 22 nm thick a-Si:H films as a function of the erosion temperature (see section 3.2).

temperature was increased in 50 K steps up to 1000 K, and AES spectra were recorded at room temperature after each anneal. The change of the film thickness versus the annealing temperature was estimated from the Si_{92}/Pt_{64} AES peak ratio. Up to a temperature of 500 K, the films were stable, and only a small decrease of the AES peak ratio was observed, probably due to the formation of a Pt silicide *at* the interface. However, above 500 K, the film thickness decreased rapidly, suggesting

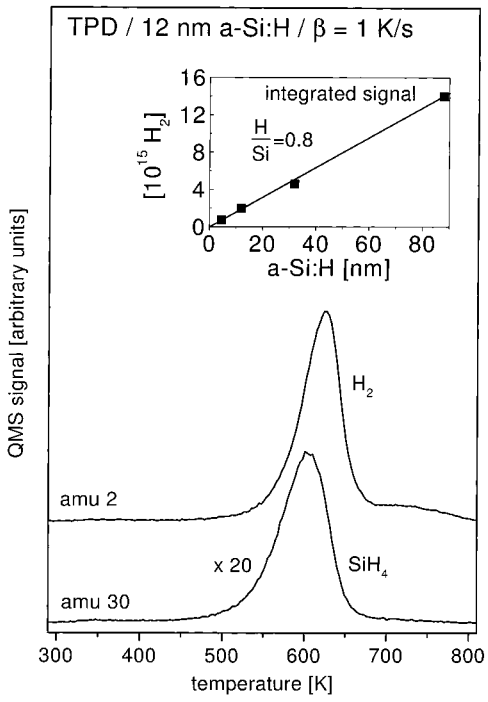

Figure 4. Hydrogen (top) and silane (bottom) signals monitored during the thermal decomposition of a 12 nm thick a-Si:H film. The inset shows the integrated hydrogen signal as a function of the film thickness.

the onset of thermally activated diffusion of Si and/or Pt. Similar findings have been reported for other a-Si:H/metal interfaces: Nemanich et al.[27] investigated the thermal stability of Pd deposited on a-Si:H and observed the formation of a bulk silicide due to Pd diffusion at temperatures above 373 K. Even Au, which does not form a silicide, was reported to diffuse into a-Si:H at temperatures as low as 473 K.[31]

From the AES results discussed above it is evident that the thermal stability of the a-Si:H/Pt(111) system is limited to approximately 500 K. To complement the AES measurement, the thermal decomposition of a-Si:H was studied by means of TDS; the films were subjected to a linear temperature ramp and the evolution of volatile products was simultaneously monitored with the QMS. Hydrogen and silane (SiH_4) were the only volatile products detected during the thermally activated decomposition of a-Si:H. Both hydrogen and silane desorption commence at 500 K and peak around 600 K (Figure 4). Molecular hydrogen is by far the dominating product: approximately 90% of the hydrogen bound to the Si network was detected in this decomposition channel. The detection of SiH_4 indicates that the a-Si:H film gets partially etched away above 500 K. The silane yield was estimated from the number of Si atoms detected in the silane channel, divided by the total number of Si atoms present in the a-Si:H films, deduced from growth rate and deposition time. Approximately 1% of the Si atoms of the a-Si:H films were detected in the SiH_4 channel. This corroborates the supposition that the decrease of the film thickness as observed with AES is due to diffusion and formation of a platinum silicide.

A comparison of the AES and the TDS data reveals that a-Si:H films on Pt(111) are stable up to 500 K, and that the silicide formation above 500 K is accompanied by the evolution of hydrogen. However, free-standing a-Si:H flakes and a-Si:H films deposited on Si wafer or glass have been reported to be stable up to at least 800 K, the onset of the crystallization.[32] The evolution of hydrogen from a-Si:H films deposited at room temperature on sapphire or crystalline silicon substrates has been

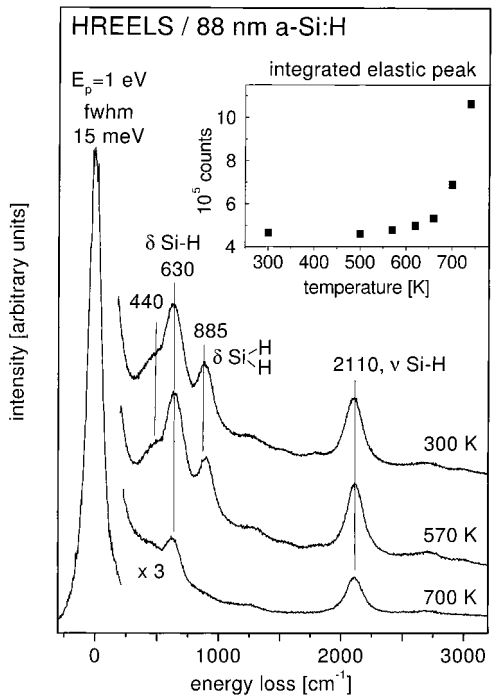

Figure 5. HREELS spectra of a 88 nm thick a-Si:H film as deposited and after annealing at the indicated temperature. The inset shows the intensity of the elastic peak versus the annealing temperature.

observed to peak around 643 and 773 K.[33,34] Likewise, hydrogen adsorbed on silicon single-crystal surfaces is stable to at least 650 K; e.g., on Si(100) the desorption of hydrogen from dihydride and monohydride states was observed at 690 and 800 K, respectively.[35] Thus, the low thermal stability of the a-Si:H films investigated in the present study has to be attributed to diffusion of Si into the substrate and formation of a platinum silicide.

Figure 4 reveals a linear increase of the integrated hydrogen signal versus the deposition time. This result suggests a uniform hydrogen concentration throughout the films. Neglecting hydrogen diffusion into the bulk, a hydrogen content of approximately 45 at. % was calculated from the integrated hydrogen desorption signal and the film thickness. Such high values of the hydrogen content are typically observed for a-Si:H films grown at low substrate temperatures and are associated with the existence of dihydride (SiH_2) groups.[36−41]

The TDS results reveal that hydrogen is bound to the Si network, but the data do not provide direct information about the bonding environment of hydrogen, i.e., the existence of monohydride and dihydride groups in the a-Si:H film. Therefore, the bonding configuration of hydrogen in the a-Si:H films was investigated by means of HREELS. The spectra of an a-Si:H film, as-deposited and after flashing to the indicated temperature, respectively, are displayed in Figure 5. The spectrum of the as-deposited film shows close resemblance to infrared (IR) spectra collected from micrometer thick a-Si:H films deposited by PECVD.[42−44] The loss features can be attributed to the Si−H stretching (2110 cm^{-1}) and wagging modes (630 cm^{-1}), and a dihydride bending/scissor mode (885 cm^{-1}). The small shoulder at 440 cm^{-1} is probably due to the Si−Si stretching mode of the network. The fact that the dihydride scissor mode was observed in the HREEL spectrum of the as-deposited a-Si:H film (Figure 5) clearly reveals the presence of dihydride surface groups. The Si−H stretching mode at 2100 cm^{-1} is commonly attributed to dihydrides or to clustered monohydrides.[42] On the other hand, Angot et al.[45] investigated an a-Si:H film with HREELS and assigned the Si−H stretching mode at 2105 cm^{-1} to monohydride surface species, because the characteristic scissor mode of dihydrides has not been observed. Thus, both monohydride and dihydride groups seem to coexist at the surface of a-Si:H.

Heating the a-Si:H film to 570 K did not change the spectral features. This result is remarkable, because this temperature is well above the onset of both silicide formation (Figure 3) and hydrogen desorption (Figure 4). Taking the surface sensitivity of HREELS into consideration, the data indicate the stability of hydride groups at the surface up to 570 K. Therefore, the hydrogen evolution seems to originate from growth of the silicide at the a-Si:H/Pt interface. The dihydride related feature disappeared only after heating the film to 700 K. At this temperature most of the Si atoms already dissolved in the Pt bulk (Figure 3).

The intensity of the elastic peak versus the annealing temperature is displayed in the insert of Figure 5. The variation of the intensity of the elastically scattered electrons can be used to monitor transitions which modify the surface roughness.[46,47] In accordance with the HREELS spectra, the development of the intensity indicates a stable surface of the a-Si:H films up to 600 K. Above this temperature the intensity increases, indicating a smoothing of the surface. A comparison with the AES results shown in Figure 3 reveals that the increase of the intensity coincides with the completion of the platinum silicide formation. This provides further evidence that the surface is stable up to temperatures clearly above the onset of diffusion, and thus proves that the platinum silicide formation starts at the Pt/a-Si:H interface and proceeds toward the surface.

The results of the experiments reported here indicate that a-Si:H films, deposited at room temperature by means of IBD, grow in two-dimensional fashion and exhibit a high hydrogen content of approximately 45 at. % bound in both monohydride and dihydride structures. The thermal stability of the films is limited to 500 K. Above this temperature, the formation of a platinum silicide at the a-Si:H/Pt(111) interface was observed.

3.2. Chemical Erosion of a-Si:H.

To study the hydrogen atom induced chemical erosion of a-Si:H, a 50 nm thick a-Si:H film was exposed to hydrogen atoms at a temperature of 300 K, and the evolution of volatile products was simultaneously monitored by means of the QMS. The data collected in the channels 28−32 amu (atomic mass unit) and 60−62 amu, respectively, are displayed in Figure 6. The shutter was opened at $t = 0$ s. The observed mass spectrometer signals are consistent with the tabulated fragmentation patterns of silane[22] and disilane,[23] respectively; higher silicon hydride species were not detected. The reaction is specific to atomic hydrogen; molecular hydrogen did not react with a-Si:H. The scaling of the signals indicates that silane is the dominant product of the etching reaction. However, the surprisingly low intensity of disilane related fragments suggests that disilane reacts with the hydrogen covered wall of the source chamber and is thus not detected efficiently.

All channels exhibit the same kinetics, i.e., a sudden jump at $t = 0$ s, followed by a slow increase; after reaching a plateau, the signals decrease again and finally vanish for prolonged exposures. The absence of an induction period after opening the shutter suggests that the products are formed in one step through the direct reaction of hydrogen atoms with the corresponding precursor species, silyl ($-SiH_3$) and disilyl ($-Si_2H_5$) surface groups, respectively. However, due to the high flux of hydrogen atoms ($\sim 10^{16}$ H cm^{-2} s^{-1}) in combination with the

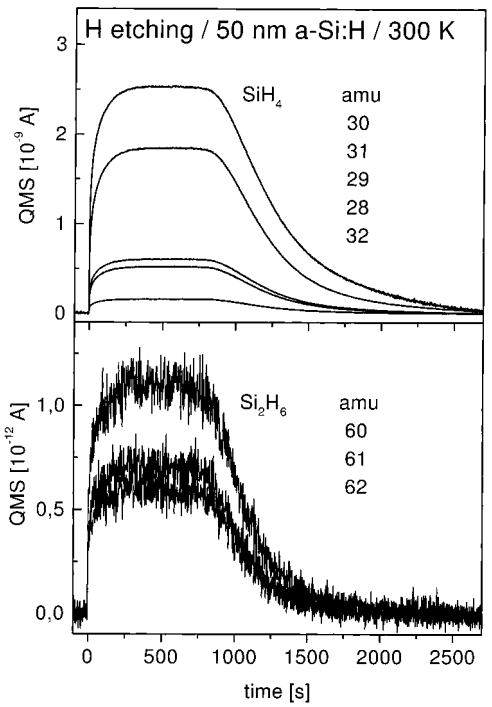

Figure 6. QMS signals monitored in the silane (top) and disilane (bottom) channels during the erosion of a 50 nm thick a-Si:H film at 300 K. The hydrogen exposure started at $t = 0$ s, using a hydrogen flux of $\sim 10^{16}$ H cm^{-2} s^{-1}.

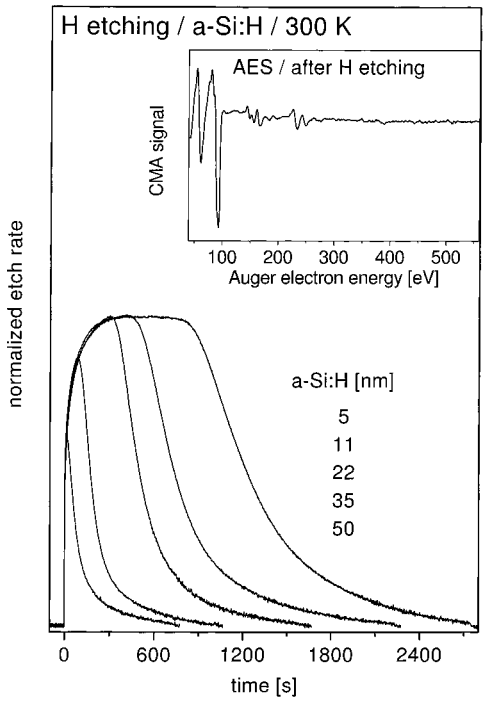

Figure 7. Erosion of 5−50 nm thick a-Si:H films at 300 K monitored in the 30 amu channel. The inset displays a typical AES spectrum collected after the hydrogen exposure.

relatively low time resolution of the experiment (the QMS was multiplexed with 1 Hz), a two-step mechanism cannot be excluded.

The decrease of the signals observed beyond the maximum of the erosion seems to be caused by the depletion of the a-Si:H film. The experiment was thus repeated with 5−50 nm thick a-Si:H films (Figure 7). The hydrogen fluence, which was necessary to observe the decay of the erosion rate, increased

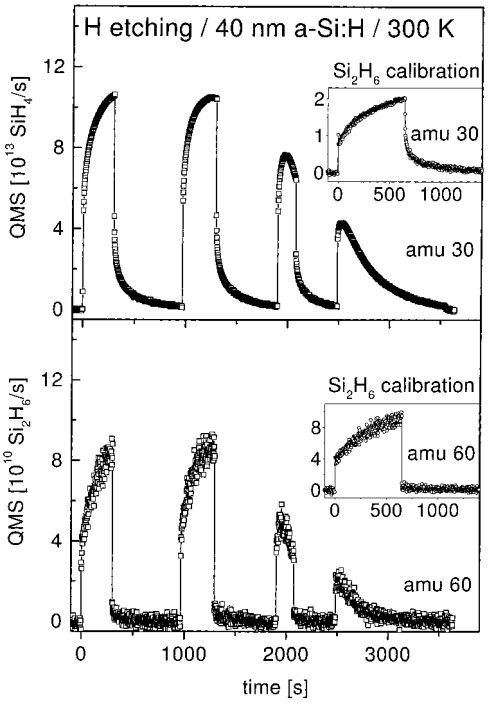

Figure 8. QMS signals monitored in the 30 (silane) and 60 amu (disilane) channels during the erosion of a 40 nm thick a-Si:H film at 300 K. The hydrogen exposure started at $t = 0$ s and was interrupted several times. The inset shows the response of the QMS signals after opening and closing the shutter while disilane was admitted to the preparation chamber.

with the thickness of the a-Si:H films (Figure 7). In addition, Auger electron spectra were collected after the silane signal decreased to the noise level (Figure 7, inset). The spectra prove that only a thin layer of a platinum silicide remained at the surface. These findings demonstrate that hydrogen atoms are capable of etching a-Si:H at room temperature.

The depletion of a-Si:H toward the end of the erosion does not cause a sudden drop in the erosion signal, but rather a slow decrease, and the tailing of the signal is more pronounced for thicker films (Figure 7). This behavior is probably related to the roughness of the a-Si:H films: during the final phase of the erosion, patches of a-Si:H will remain on the otherwise bare Pt substrate, leading to the observed tailing of the signal. The roughness of the films, which may originate from either the deposition or the erosion, seems to increase with the film thickness. Likewise, an increase of the surface roughness of a-Si:H films, from 3 to 5 nm, with increasing film thickness, ranging from 1 to 50 nm, has been observed with STM.[48]

It is tempting to assume that the slow increase of the silane signal, observed after the initial jump of the erosion rate at zero time (Figure 6), reflects the kinetics of the regeneration of the precursor species, e.g., the formation of $-SiH_3$ surface groups via hydrogenation of SiH_2. Therefore, to assist in the interpretation of the experimentally observed kinetics, the response of the erosion signals to an interrupted flux of hydrogen atoms was investigated (Figure 8). This procedure allows us to discriminate between transient signals which were induced by the characteristics of our detection system and those reflecting the kinetics of the etching reaction. An inspection of Figure 8 reveals that the disilane signal (60 amu) immediately drops to zero after closing the shutter, whereas the silane signal (30 amu) decreases exponentially, indicating desorption of silane from the walls of the source chamber.

The interaction of the erosion products with the atom source was thus investigated in separate experiments. Silane and

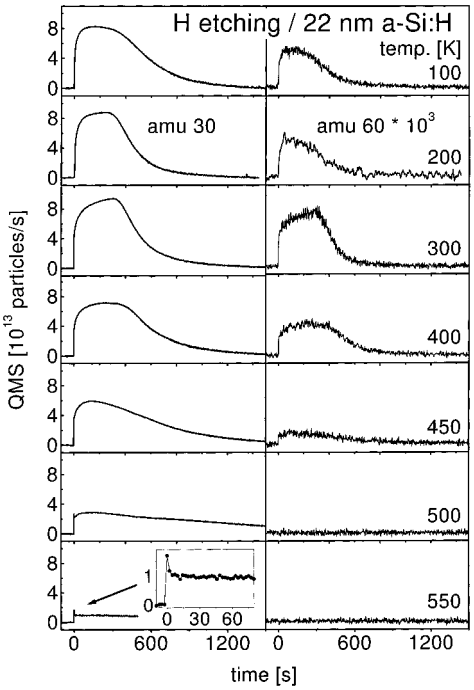

Figure 9. QMS signals monitored in the 30 (SiH_4) and 60 amu (Si_2H_6) channels during the erosion of a-Si:H films as a function of film temperature. All a-Si:H films were initially 22 nm thick.

disilane were admitted to the preparation chamber through leak valves, and the response of the QMS in both the silane and the disilane channels was monitored while opening and closing the shutter. For silane only the expected steplike variation of the 30 amu signal was observed, regardless whether the atom source was switched on or off (not shown). Likewise, disilane produced steplike variations in the 30 and 60 amu channels, if the atom source was not in operation (not shown). In the presence of hydrogen atoms, however, an interrupted flux of disilane produced features similar to those observed during the erosion of a-Si:H: both the 30 and 60 amu signals exhibit a sudden jump after opening the shutter, followed by a slow increase and finally reaching a plateau; after closing the shutter the 60 amu signal immediately drops to zero, whereas the 30 amu signal decays exponentially (Figure 8, inserts). The transients in the signals reflect the change of disilane sticking coefficient on the wall of the source chamber as a function of the wall condition, and the reaction of adsorbed disilane toward silane, probably via silyl groups. Thus, only the sudden jump of the signals after opening the shutter reflects the kinetics of the erosion reaction.

A quantitative analysis of the data reveals that approximately 25% of the silane signal, which was detected during the erosion of a-Si:H, originates from the erosion product disilane and its conversion to silane on the hydrogen covered wall of the source chamber. However, the disilane-to-silane conversion is not sufficient to explain the observed transients in the 30 amu channel; additionally, the formation of higher silicon hydride species Si_xH_y ($x \geq 3$) has thus to be postulated. These species were not directly detected, but contribute to ~25% of the observed silane signal. The desorption of higher silicon hydrides has been observed from a hydrogen covered Si(100) surface.[14]

The temperature dependence of etching reaction was investigated by exposing a-Si:H films to hydrogen atoms at various temperatures. All films were deposited at 300 K. The silane (30 amu) and disilane (60 amu) signals monitored during the erosion of the a-Si:H films are displayed in Figure 9. Knowing the flux of hydrogen atoms and the sensitivity of the QMS, the

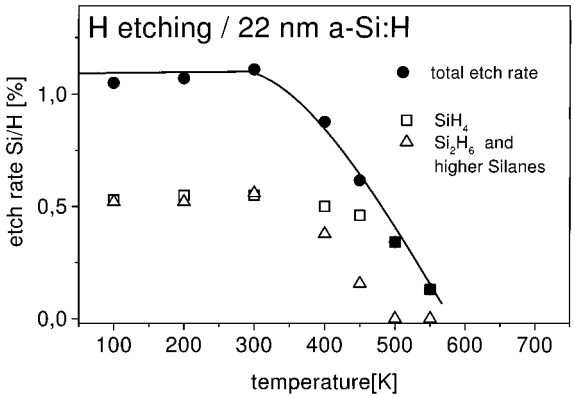

Figure 10. Fraction of silicon atoms detected in the SiH_4 and $Si_{\geq 2}H_y$ channels during the erosion of a-Si:H versus erosion temperature. All a-Si:H films were initially 22 nm thick.

amount of silicon atoms, which were removed from the film through the formation of silane and disilane, respectively, was calculated from those data (Figure 3). The corresponding erosion rates are displayed in Figure 10.

Between 100 and 300 K, similar maximum values of the silane and disilane signals were observed after the "induction" period, corresponding to an etching rate of approximately 0.01 per incoming hydrogen atom (Figure 10). Approximately equal amounts of silicon atoms were removed from the film through the formation of silane and higher silicon hydrides ($Si_{\geq 2}H_y$), respectively. However, it has to be pointed out that a continuous erosion at or below 200 K was only observed after exceptional care was taken to reduce oxygen and carbon contaminations. Otherwise, the erosion stopped after prolonged hydrogen exposures with the Pt(111) surface still covered with a-Si:H. On such samples AES spectra revealed the presence of carbon and oxygen as surface impurities.

Above 300 K, the etching rate starts to decrease, first observed in the disilane channel, later also in the silane channel. To observe a stationary erosion, the precursor species of the erosion products have to be continuously regenerated through reactions of hydrogen atoms with a-Si:H. Likely precursor candidates are silyl ($-SiH_3$) and disilyl ($-Si_2H_5$) surface groups, generated through hydrogenation and insertion reactions. The decreasing erosion signals above 300 K thus provide evidence for the commencing thermal instability of higher hydrides, in particular polymer-like film structures.

Above 450 K, the formation of disilane ceased, and the 30 amu signal exhibits a more steplike increase after opening the shutter. The sudden jump of the silane signal at $t = 0$ s suggests that the formation of silane proceeds via a direct interaction of silyl and hydrogen atoms: $H(g) + -SiH_3(ad) \rightarrow SiH_4(g)$. The absence of an "induction" period provides further evidence that the transients in the erosion signals, which were observed at lower temperatures, have be attributed to the kinetics of the disilane-to-silane conversion on the initially hydrogen covered walls of the source chamber. From the AES data shown in Figure 3, it is evident that diffusion and silicide formation are slow processes below 500 K. This is confirmed by the evaluation of the erosion signals, which reveals that even at 450 K 85% of the silicon atoms of the a-Si:H film were removed through the erosion channel and detected as silane and disilane in the gas phase.

However, above 500 K, diffusion and silicide formation compete with the etching reaction. Accordingly, only a small fraction of the silicon atoms of the film was detected in the gas phase (Figure 3). Due to the absence of disilane formation, the

silane signal shows a true steplike increase after opening the shutter. In addition, a small spike was observed at $t = 0$ s (Figure 9, insert). This feature suggests the presence of silyl surface groups after deposition of a-Si:H. After opening the shutter, these groups immediately react toward silane. However, the regeneration of silyl groups appears to be the rate-limiting step above 500 K, causing the spike-like feature of the erosion signal.

The results of the etching experiments reported here show that the hydrogen induced chemical erosion of polymer-like a-Si:H films proceeds via the formation of silane, disilane, and higher silicon hydride species. Silane and disilane were unambiguously identified by means of QMS. The sudden jump of the erosion signals after opening the shutter and the observed temperature dependence suggest that the products are formed in a direct reaction of hydrogen atoms with silyl and disilyl surface groups, respectively. The constant etching rate observed below 300 K reveals a small activation barrier for the rate-determining step of the erosion reaction.

The kinetics of the corresponding gas-phase reactions suggests that the formation of silane/disilane is initiated by the addition of hydrogen to the silyl/disilyl precursor group via a frontside attack, followed by the cleavage of the Si−Si bond.[49] In the gas phase, the hydrogen induced cleavage of a Si−Si bond typically exhibits a low activation barrier of approximately 0.1 eV.[50] Whether the reaction proceeds via a hot atom or an Eley−Rideal mechanism could not be decided on the basis of the experimental results. However, a molecular dynamics trajectory calculation of the hydrogen abstraction on monohydride surface of Si(001) suggested the operation of a hot atom mechanism.[51] Recently, the existence of trapped, thermally nonequilibrated hydrogen atoms on the silicon surface was demonstrated by Dinger et al.[35] However, the observation of an enhanced silane signal immediately after opening the shutter at temperatures above 450 K indicates that the abstraction of SiH_3 is not the rate limiting reaction step, at least at high temperatures.

Earlier investigations of the chemical erosion of porous silicon[52] and Si(100)[53] provided evidence that the formation of silane proceeds via a Langmuir−Hinshelwood (LH) mechanism. Glass et al.[52] studied the formation and thermal stability of silicon hydride species on porous silicon by Fourier transform infrared spectroscopy, and concluded that the LH disproportionation reaction of SiH_3 and SiH_x species leads to the formation of silane, $SiH_3 + SiH_x \rightarrow SiH_4 + SiH_{x-1}$. This mechanism suggests an increasing erosion rate with increasing erosion temperature, in disagreement with the data shown in Figure 10. However, the present study investigated the stationary erosion of a-Si:H, i.e., using a constant supply of hydrogen atoms, and under these reaction conditions the temperature dependence of the SiH_4 formation is consistent with a direct reaction (Eley−Rideal or hot atom) between incoming hydrogen atoms and SiH_3 precursor species, $H + SiH_3 \rightarrow SiH_4$, limited by the supply of SiH_3 groups. Similar results were reported for the stationary erosion of crystalline silicon:[13,15,18] the temperature dependence of the etching reaction of Si(100)[18] closely resembles that observed in the present study. Similarly, a decrease of the erosion rate with increasing temperature, from 350 K to approximately 1000 K, has also been reported for the reaction of atomic hydrogen with Si(111).[13,15] However, in none of these studies the formation of disilane has been observed.

The fast erosion observed below 300 K is at odds with the findings of Chiang et al.,[19] who observed no or only very slow erosion below 373 K. As mentioned above, we also observed a decreasing erosion rate for prolonged hydrogen exposures below 300 K if oxygen and/or carbon surface impurities exceeded a certain limit. At temperatures below 300 K, a slow erosion has thus to be attributed to the formation of silicon oxides and/or carbides, which are inert regarding the hydrogen induced erosion *below* 300 K. At or above room temperature, the carbide and/or oxide impurities are obviously removed through the interaction with hydrogen atoms, suggesting the existence of a thermally activated reaction step. As a consequence, the previously reported lack of erosion at low temperatures[19] does not necessarily indicate that formation of silane proceeds via a Langmuir−Hinshelwood mechanism.

The erosion experiment at 550 K, i.e., the spike of the silane signal observed immediately after opening the shutter, reveals that the formation of silane via the hydrogen induced abstraction of silyl is a fast reaction even at 550 K. This is in accordance with the results of Jo et al.,[17] who prepared silyl groups on Si(100) via dissociative adsorption of disilane, and observed a fast reaction of adsorbed silyl toward silane at 480 K. The rate-limiting step at higher temperatures can thus be identified as the formation of silyl surface groups, probably via the hydrogenation of dihydride surface groups: $SiH_2(ad) + H(g) \rightarrow SiH_3(ad)$. On the other hand, dihydride surface groups appear to be stable up to at least 570 K as demonstrated by the HREELS result shown in Figure 5.

The postdeposition treatment of a-Si:H films with atomic hydrogen, termed "chemical annealing", allows preparation of microcrystalline silicon films with improved electronic properties at low substrate temperatures.[6−9] Chemical annealing is usually performed at temperatures between 400 and 600 K and results in silicon films with a reduced hydrogen content,[7,8] an increased stability against light-induced degradation,[7] and an increased crystallinity.[6,9] In this temperature range the erosion yield starts to decrease (Figure 10), thus suggesting a competition between the generation of SiH_3 groups via insertion of hydrogen into Si−Si bonds and the thermally activated elimination of H_2 from SiH_x surface groups, leading to the formation of new Si−Si bonds. The balance between the preferential insertion of hydrogen into strained Si−Si bonds and the preferential formation of unstrained Si−Si bonds explains the relaxation of the silicon network observed during chemical annealing.

4. Conclusions

a-Si:H films deposited by means of the IBD method at 300 K on a Pt(111) single crystal exhibit polymer-like features, i.e., a hydrogen content of approximately 45 at. % bound in monohydride and dihydride groups. The films grow in a two-dimensional fashion, and the roughness increases with the film thickness. The thermal stability of the films is limited to 500 K by the formation of a platinum silicide, which commences at a-Si:H/Pt interface and proceeds toward the surface. The decomposition of a-Si:H in the course of the silicide formation is accompanied by the evolution of molecular hydrogen, accounting for 90% of the hydrogen, and silane around 600 K.

Atomic hydrogen reacts with polymer-like a-Si:H films toward silane, disilane, and higher silicon hydride species. Between 100 and 300 K, the erosion yield is constant and exhibits a maximum of approximately 1% with about equal contributions from silane and higher silicon hydrides, respectively. Above 300 K, the erosion rate was observed to decrease, first in the disilane channel, and above 400 K also in the silane channel. The formation of both silane and disilane is not thermally activated and proceeds via a direct interaction of atomic hydrogen and the corresponding precursor species, silyl and disilyl surface groups, respectively. The rate is limited by

the regeneration and thermal stability of the precursor groups, at least at temperatures above 400 K.

Acknowledgment. The authors are grateful to T. Schwarz-Selinger and M. Meier for supporting the calibration of the hydrogen flux of the atom source.

References and Notes

(1) Kuo, Y.; Okajima, M.; Takeichi, M. *IBM J. Res. Dev*. **1999**, *43*, 73.
(2) Tanaka, K.; Maruyama, E.; Shimada, T.; Okamoto, H. *Amorphous Silicon*; John Wiley & Sons: Chichester, 1999.
(3) Bruno, G.; Capezzuto, P.; Madan, A. *Plasma deposition of amorphous silicon-based materials*; Academic Press: San Diego, CA, 1995.
(4) Shirai, H.; Arai, T. *J. Non-Cryst. Solids* **1996**, *198*−*200*, 931.
(5) An, I.; Li, Y. M.; Wronski, C. R.; Collins, R. W. *Phys. Rev. B* **1993**, *48*, 4464.
(6) Shimizu, I. *J. Non-Cryst. Solids* **1989**, *114*, 145.
(7) Shirai, H.; Das, D.; Hanna, J.; Schimizu, I. *Appl. Phys. Lett.* **1991**, *59*, 1096.
(8) Gertkemper, Th.; Ristein, J.; Ley, L. *J. Non-Cryst. Solids* **1993**, *164*−*166*, 123.
(9) Boland, J. J.; Parsons, G. N. *Science* **1992**, *256*, 1304.
(10) Nguyen, H. V.; An, I.; Collins, R. W.; Lu, Y.; Wakagi, M.; Wronski, C. R. *Appl. Phys. Lett.* **1994**, *65*, 3335.
(11) Turban, G.; Catherine, Y.; Grolleau, B. *Thin Solid Films* **1981**, *77*, 287.
(12) Jasinski, J. M. *Chem. Phys. Lett.* **1993**, *211*, 564.
(13) Olander, D. R.; Balooch, M.; Abrefah, J.; Siekhaus, W. J. *J. Vac. Sci. Technol., B* **1987**, *5*, 1404.
(14) Gates, S. M.; Kunz, R. R.; Greenlief, C. M. *Surf. Sci.* **1989**, *207*, 364.
(15) Abrefah, J.; Olander, D. R. *Surf. Sci*. **1989**, *209*, 291.
(16) Chuang, M.-C.; Coburn, J. W. *J. Vac. Sci. Technol., A* **1990**, *8*, 1969.
(17) Jo, S. K.; Gong, B.; Hess, G.; White, J. M.; Ekerdt, J. G. *Surf. Sci.* **1997**, *394*, L162.
(18) Dinger, A.; Lutterloh, C.; Küppers, J. *Chem. Phys. Lett*. **2000**, *320*, 405.
(19) Chiang, C.-M.; Gates, S. M.; Lee, S. S.; Kong, M.; Bent, S. F. *J. Phys. Chem. B* **1997**, *101*, 9537.
(20) Schwarz-Selinger, T.; von Keudell, A.; Jacob, W. *J. Vac. Sci. Technol*., *A* **2000**, *18*, 995.
(21) Musket, R. G.; McLean, W.; Colmenares, C. A.; Makowiecki, D. M.; Siekhaus, W. J. *Appl. Surf. Sci.* **1982**, *10*, 143.
(22) *NIST Chemistry Webbook*; http://webbook.nist.gov/chemistry.
(23) Ring, M. A.; Beverly, G. D.; Koester, F. H.; Hollandsworth, R. P. *Inorg. Chem.* **1969**, *8*, 2033.
(24) Ertl, G.; Küppers, J. *Low Energy Electrons and Surface Chemistry*; VCR: Weinheim, 1985.
(25) Murarka, S. P.; Kinsbron, E.; Fraser, D. B.; Andrews, J. M.; Lloyd, E. J. *J. Appl. Phys*. **1983**, *54*, 6943.
(26) Saenger, K. L.; Grill, A.; Kotecki, D. E. *J. Appl. Phys*. **1998**, *83*, 802.
(27) Nemanich, R. J.; Tsai, C. C.; Thompson, M. J.; Sigmon, T. W. *J. Vac. Sci. Technol*. **1981**, *19*, 685.
(28) Ibach, H.; Rowe, J. E. *Surf. Sci*. **1973**, *9*, 1951.
(29) Yu, H.; Leung, K. T. *Surf. Sci*. **1999**, *432*, 245.
(30) Antoine, A. M.; Drévillon, B.; Roca i Cabarrocas, P. *J. Non-Cryst. Solids* **1985**, *77&78*, 769.
(31) Tsai, C. C.; Nemanich, R. J.; Thompson, M. J. *J. Vac. Sci. Technol*. **1982**, *21*, 632.
(32) Shao, W.-L.; Shinar, J.; Gerstein, B. C.; Li, F.; Lannin, J. S. *Phys. Rev. B* **1990**, *41*, 9491.
(33) Beyer, W.; Wagner, H. *J. Appl. Phys.* **1982**, *53*, 8745.
(34) Bayer, W.; Wagner, H. *J. Non-Cryst. Solids* **1983**, *59&60*, 161.
(35) Dinger, A.; Lutterloh, C.; Küppers, J. *Chem. Phys. Lett*. **1999**, *311*, 202.
(36) Alpuim, P.; Chu, V.; Conde, J. P. *J. Appl. Phys*. **1999**, *86*, 3812.
(37) Kessels, W. M. M.; Severens, R. J.; van de Sanden, M. C. M.; Schram, D. C. *J. Non-Cryst. Solids* **1998**, *227*−*230*, 133.
(38) Hishikawa, Y.; Tsuge, S.; Nakamura, N.; Tsuda, S.; Nakano, S.; Kuwano, Y. *J. Appl. Phys*. **1991**, *69*, 508.
(39) Tsai, C. C.; Anderson, G. B.; Thompson, R. *J. Non-Cryst. Solids* **1991**, *137&138*, 673.
(40) Roca i Cabarrocas, P. *Appl. Phys. Lett.* **1994**, *65*, 1674.
(41) Baum, J.; Gleason, K. K.; Pines, A.; Garroway, A. N.; Reimer, J. A. *Phys. Rev. Lett*. **1986**, *56*, 1377.
(42) Langford, A. A.; Fleet, M. L.; Nelson, B. P.; Lanford, W. A.; Maley, N. *Phys. Rev. B* **1992**, *45*, 13367.
(43) Srinivasan, E.; Lloyd, D. A.; Parsons, G. N. *J. Vac. Sci. Technol., A* **1997**, *15*, 77.
(44) Miyoshi, Y.; Yoshida, Y.; Miyazaki, S.; Hirose, M. *J. Non-Cryst. Solids* **1996**, *198*−*200*, 1029.
(45) Angot, T.; Chelly, R. *Surf. Sci*. **1998**, *402*−*404*, 52.
(46) Tautz, F. S.; Schaefer, J. A. *J. Appl. Phys.* **1998**, *84*, 6636.
(47) Hess, G.; Russell, M.; Gong, B.; Parkinson, P.; Ekerdt, J. G. *J. Vac. Sci. Technol., A* **1997**, *15*, 1129.
(48) Tanenbaum, D. M.; Laracuente, A. L.; Gallagher, A. *Phys. Rev. B* **1997**, *56*, 4243.
(49) Fabry, L.; Potzinger, P.; Reimann, B.; Ritter, A.; Steenbergen, H. P. *Organometallics* **1986**, *5*, 1231.
(50) Ellul, R.; Potzinger, P.; Reimann, B. *J. Phys. Chem*. **1984**, *88*, 2793.
(51) Kratzer, P. *Chem. Phys. Lett.* **1998**, *288*, 396.
(52) Glass, J. A., Jr.; Wovchko, E. A.; Yates, J. T., Jr. *Surf. Sci*. **1996**, *348*, 325.
(53) Cheng, C. C.; Yates, J. T., Jr. *Phys. Rev. B* **1991**, *43*, 4041.